



ELSEVIER

Contents lists available at ScienceDirect

## Cerebral Circulation - Cognition and Behavior

journal homepage: [www.elsevier.com/locate/cccb](http://www.elsevier.com/locate/cccb)

## Zooming in on cerebral small vessel function in small vessel diseases with 7T MRI: Rationale and design of the “ZOOM@SVDs” study



Hilde van den Brink<sup>a</sup>, Anna Kopczak<sup>b</sup>, Tine Arts<sup>c</sup>, Laurien Onkenhout<sup>a</sup>, Jeroen C.W. Siero<sup>c,d</sup>, Jaco J.M. Zwanenburg<sup>c</sup>, Marco Duering<sup>b,e,f</sup>, Gordon W. Blair<sup>g</sup>, Fergus N. Doubal<sup>g</sup>, Michael S. Stringer<sup>g</sup>, Michael J. Thrippleton<sup>g</sup>, Hugo J. Kuijff<sup>h</sup>, Alberto de Luca<sup>a,g</sup>, Jeroen Hendrikse<sup>c</sup>, Joanna M. Wardlaw<sup>g</sup>, Martin Dichgans<sup>b,e,f</sup>, Geert Jan Biessels<sup>a,\*</sup>, on behalf of the SVDs@target group

<sup>a</sup> Department of Neurology and Neurosurgery, UMC Utrecht Brain Center, University Medical Center Utrecht, Heidelberglaan 100, Utrecht, 3508 GA, the Netherlands

<sup>b</sup> Institute for Stroke and Dementia Research, University Hospital, Ludwig-Maximilians-Universität, Munich, Germany

<sup>c</sup> Department of Radiology, Center for Image Sciences, University Medical Center Utrecht, Utrecht, the Netherlands

<sup>d</sup> Spinoza Centre for Neuroimaging Amsterdam, Amsterdam, the Netherlands

<sup>e</sup> Munich Cluster for Systems Neurology (SyNergy), Munich, Germany

<sup>f</sup> German Center for Neurodegenerative Disease (DZNE), Munich, Germany

<sup>g</sup> Brain Research Imaging Centre, Centre for Clinical Brain Sciences, UK Dementia Research Institute Centre at the University of Edinburgh, Edinburgh, United Kingdom

<sup>h</sup> Image Sciences Institute, University Medical Center Utrecht, Utrecht, the Netherlands

## ARTICLE INFO

## Keywords:

Cerebral small vessel disease  
Sporadic SVD  
CADASIL  
Stroke  
High field strength MRI  
Small vessel function

## ABSTRACT

**Background:** Cerebral small vessel diseases (SVDs) are a major cause of stroke and dementia. Yet, specific treatment strategies are lacking in part because of a limited understanding of the underlying disease processes. There is therefore an urgent need to study SVDs at their core, the small vessels themselves.

**Objective:** This paper presents the rationale and design of the ZOOM@SVDs study, which aims to establish measures of cerebral small vessel dysfunction on 7T MRI as novel disease markers of SVDs.

**Methods:** ZOOM@SVDs is a prospective observational cohort study with two years follow-up. ZOOM@SVDs recruits participants with Cerebral Autosomal Dominant Arteriopathy with Subcortical Infarcts and Leukoencephalopathy (CADASIL,  $N = 20$ ), sporadic SVDs ( $N = 60$ ), and healthy controls ( $N = 40$ ). Participants undergo 7T brain MRI to assess different aspects of small vessel function including small vessel reactivity, cerebral perforating artery flow, and pulsatility. Extensive work-up at baseline and follow-up further includes clinical and neuropsychological assessment as well as 3T brain MRI to assess conventional SVD imaging markers. Measures of small vessel dysfunction are compared between patients and controls, and related to the severity of clinical and conventional MRI manifestations of SVDs.

**Discussion:** ZOOM@SVDs will deliver novel markers of cerebral small vessel function in patients with monogenic and sporadic forms of SVDs, and establish their relation with disease burden and progression. These small vessel markers can support etiological studies in SVDs and may serve as surrogate outcome measures in future clinical trials to show target engagement of drugs directed at the small vessels.

**Abbreviations:** ASL, Arterial Spin Labeling; BOLD, Blood Oxygenation Level-Dependent; CADASIL, Cerebral Autosomal Dominant Arteriopathy with Leukoencephalopathy and Subcortical Infarcts; CDR, Clinical Dementia Rating scale; CERAD+, Consortium to Establish a Disease Registry for Alzheimer's Disease Plus battery; CES-D, Center for Epidemiologic Studies Depression Scale; CO<sub>2</sub>, Carbon Dioxide; CSF, Cerebrospinal Fluid; DTI, Diffusion Tensor Imaging; EPIC, European Prospective Investigation into Cancer and Nutrition; EtCO<sub>2</sub>, End-tidal Carbon Dioxide; fMRI, Functional Magnetic Resonance Imaging; FLAIR, Fluid Attenuated Inversion Recovery; FOV, Field Of View; FWHM, Full-Width-at-Half-Maximum; GE, Gradient Echo; GM, Grey Matter; GPRS, General Packet Radio Service; HRF, Hemodynamic Response Function; LMU, Ludwig-Maximilians-Universität; MMSE, Mini-Mental State Examination; NAWM, Normal Appearing White Matter; NIHSS, National Institute for Health Stroke Scale; PI, Pulsatility Index; ROI, Region Of Interest; SPPB, Short Physical Performance Battery; SVDs, Small Vessel Diseases; SWI, Susceptibility Weighted Imaging; TE, Echo Time; TI, Inversion Time; TR, Repetition Time; TSE, Turbo Spin Echo; UMCU, University Medical Center Utrecht; V<sub>max</sub>, Maximum velocity; V<sub>min</sub>, Minimum velocity; V<sub>mean</sub>, Mean velocity; WM, White Matter; WMH, White Matter Hyperintensity.

\* Corresponding author.

E-mail address: [g.j.biessels@umcutrecht.nl](mailto:g.j.biessels@umcutrecht.nl) (G.J. Biessels).

<https://doi.org/10.1016/j.cccb.2021.100013>

Received 18 February 2021; Received in revised form 14 April 2021; Accepted 15 April 2021

Available online 24 April 2021

2666-2450/© 2021 The Author(s). Published by Elsevier B.V. This is an open access article under the CC BY-NC-ND license (<http://creativecommons.org/licenses/by-nc-nd/4.0/>)

## 1. Introduction

Cerebral small vessel diseases (SVDs) affect small arteries, capillaries and small veins in the brain [1]. SVDs account for most hemorrhagic strokes, a quarter of ischemic strokes, and at least 40% of dementia cases, alone or in combination with neurodegenerative pathology [1]. Roughly 70% of 65-year-old individuals and almost all 90-year-olds exhibit manifestations of SVDs on brain imaging [2]. Despite this profound impact, there is no specific treatment for SVDs with proven efficacy. Current management is limited to treatment of risk factors, foremost hypertension, which is clearly of fundamental importance, but is not sufficient to halt SVDs and their consequences. Better insight into the mechanisms underlying SVDs is urgently needed to support the development of targeted treatments.

Over the years there has been major progress in the development of SVD biomarkers. These include visible manifestations on MRI (i.e. lacunes, white matter hyperintensities, microbleeds, enlarged perivascular spaces [3]), more subtle microstructural white matter changes (measured with diffusion tensor imaging [4–6]) and blood-based biomarkers of neuro-axonal damage (serum neurofilament light [7]). All of these biomarkers primarily reflect SVDs-related parenchymal injury. This injury relates to important functional outcomes, in particular cognitive decline and dementia, but is essentially a downstream consequence of a disease that originates in the small cerebral vessels. In these vessels, SVDs manifest as loss of smooth muscle cells, fibrinoid necrosis, narrowing of the lumen, and thickening of the vessel wall [1,8]. This impacts vessel function, as observed in pial and parenchymal arteries in experimental animal models of both hereditary and sporadic forms of SVDs [9,10]. Emerging techniques at 7T MRI provide noninvasive measures of cerebral small vessel function in humans [11]. These measures allow SVDs to be studied at their core, the small vessels themselves, and have important potential as biomarker of SVDs to help unravel the pathophysiology and serve as surrogate outcome measures in treatment studies.

This paper presents the rationale and design of ZOOM@SVDs, part of the SVDs@target research program (see textbox). ZOOM@SVDs explores (1) which aspects of small vessel function on 7T brain MRI are affected in patients with Cerebral Autosomal Dominant Arteriopathy with Subcortical Infarcts and Leukoencephalopathy (CADASIL) and in patients with symptomatic sporadic SVD, and (2) how small vessel function relates to SVD severity at baseline and disease progression after two years.

---

**SVDs@target** (Small vessel diseases in a mechanistic perspective: Targets for Intervention – Affected pathways and mechanistic exploitation for prevention of stroke and dementia) ([www.svds-at-target.eu](http://www.svds-at-target.eu)). The program is funded by Horizon 2020 and includes three clinical studies: ZOOM@SVDs (current paper), INVESTIGATE-SVDs, and TREAT-SVDs. This textbox provides a summary on INVESTIGATE-SVDs and TREAT-SVDs.

**INVESTIGATE-SVDs** (Imaging NeuroVascular, Endothelial and Structural Integrity in preparation to Treat Small Vessel Diseases.): PI Prof JM Wardlaw, Centre for Clinical Brain Sciences Edinburgh.

INVESTIGATE-SVDs is a three-centre (Edinburgh, Maastricht, Munich) observational study in 45 patients with sporadic SVDs and in 30 patients with CADASIL. The main objective is to advance knowledge of SVD pathophysiology by assessing the relationship between blood brain barrier integrity, cerebrovascular reactivity to CO<sub>2</sub>, intracranial vascular and CSF pulsatility, blood pressure and its variability and clinical and structural features of SVD.

**TREAT-SVDs** (Effects of Amlodipine and other Blood Pressure Lowering Agents on Microvascular Function in Small Vessel Diseases): PI Prof M Dichgans, Institute for Stroke and Dementia Research, Ludwig-Maximilians-Universität, Munich

TREAT-SVDs is a five-centre (Edinburgh, Maastricht, Munich, Oxford, Utrecht), randomized, open-label, crossover trial in 75 patients with sporadic SVDs and 30 patients with CADASIL. The primary objective is to test the hypothesis that the calcium channel blocker amlodipine has a beneficial effect on small vessel function in patients with symptomatic SVDs when compared to either the Angiotensin II type 1 receptor blocker losartan or the beta-blocker atenolol. The secondary objective is to test the hypothesis that losartan has a beneficial effect on small vessel function compared to atenolol.

---

## 2. Material and methods

### 2.1. Study design

ZOOM@SVDs is a prospective observational cohort study with a follow-up measurement after two years. The study is a collaboration between the University Medical Center Utrecht (UMCU) in the Netherlands and the Institute for Stroke and Dementia Research at Ludwig-Maximilians-Universität (LMU), Munich, Germany. At the UMCU, 60 patients with symptomatic sporadic SVD and 30 age and sex-matched controls are recruited. At the LMU, 20 patients with CADASIL and 10 age and sex-matched controls are recruited. Participants attend two baseline visits and one follow-up visit after two years, see Table 1 for an overview of the data collection per visit. The 7T MRI scan for all participants is performed at the UMCU. All other assessments for the patients with CADASIL and their controls are performed at the LMU.

### 2.2. Ethical approval

The Medical Ethics Review Committees of the UMCU and the LMU both approved the study (under number NL62090.041.17 and 17–088 respectively). The study is registered in the Netherlands Trial Register (under number NTR6265) and is conducted in accordance with the declaration of Helsinki and the European law of General Data Protection Regulation. Written informed consent is obtained from all participants prior to enrollment in the study.

### 2.3. Participants

Patients with symptomatic sporadic SVDs ( $N = 60$ ) are recruited from the stroke, rehabilitation and memory clinics of the UMCU, and from referring neighboring clinics (Diakonessenhuis Zeist and Utrecht). Patients with a diagnosis of CADASIL ( $N = 20$ ), either confirmed by molecular genetic testing of the *NOTCH3* gene or by skin biopsy, are recruited through the Institute for Stroke and Dementia Research at the LMU. The institute is a tertiary national referral center for patients with CADASIL in Germany. Controls are recruited among partners or relatives of the patients, and through flyer advertisement. Table 2 lists specific participant inclusion and exclusion criteria.

### 2.4. Baseline assessment

#### 2.4.1. Clinical assessment

The following measures are collected during the clinical assessment:

- Demographic factors, including age, sex and education level
- Medical history, including history of TIA, stroke, cognitive impairment and vascular risk factors (i.e. hypertension, hyperlipidemia, diabetes, smoking, BMI and alcohol use)
- Physical activity (i.e. EPIC Physical Activity Questionnaire [12]) and physical performance (i.e. SPPB [13])
- Physical examination, including a National Institute of Health Stroke Scale (NIHSS) examination [14] and blood pressure measurements
- Current medication

#### 2.4.2. Blood sampling

Laboratory investigations are performed in blood from a venipuncture in order to document the cardiovascular risk profile, including total cholesterol, HDL-cholesterol, LDL-cholesterol, triglycerides, HbA1c, and C-reactive protein. In women of childbearing age, a pregnancy test is performed as a screening measure before undergoing MRI.

In addition to these laboratory tests, blood is obtained in two 8 ml cell preparation tubes with sodium citrate (BD, 362,782). Directly after collection, peripheral blood mononuclear cells are isolated and stored at  $-80^{\circ}\text{C}$  Celsius [15], with the aim to explore the contribution of immune cells to the severity of SVDs. This procedure is also performed in the other clinical studies of SVDs@target (i.e. INVESTIGATE-SVDs and

**Table 1**  
Overview of data collection per visit.

	Baseline visit 1 Day 1	Baseline visit 2 Day 8–28	Follow-up 2 years
Informed consent	X		
Clinical assessment	X		X
Blood sampling	X		
Neuropsychological assessment	X		X
7-day blood pressure monitoring	X		
3T brain MRI	X		X
7T brain MRI		X	

**Table 2**  
Inclusion and exclusion criteria for patients with sporadic SVDs, CADASIL and healthy controls.

<b>General selection criteria for all groups</b>	
<b>Inclusion criteria</b>	<b>Exclusion criteria</b>
<ul style="list-style-type: none"> <li>- Age 18 years or older</li> <li>- Capacity to give written informed consent</li> <li>- Independent in activities of daily living (Modified Rankin score <math>\leq 3</math>)</li> </ul>	<ul style="list-style-type: none"> <li>- Pregnant or breastfeeding women and women of childbearing age not taking contraception</li> <li>- Contraindication to MRI or unable to undergo MRI protocol due to physical condition</li> <li>- Other major neurological or psychiatric conditions affecting the brain and interfering with the study design (e.g. multiple sclerosis, Parkinson's disease)</li> <li>- Life expectancy <math>&lt; 2</math> years</li> </ul>
<b>Additional selection criteria specific to patients with sporadic SVDs</b>	
<b>Inclusion criteria</b>	<b>Exclusion criteria</b>
History of a clinical lacunar stroke in the last 5 years with a corresponding small subcortical infarct visible on MRI or CT, compatible with the clinical syndrome OR Cognitive impairment defined as visiting a memory clinic with cognitive complaints and objective cognitive impairment (based on a validated cognitive measurement tool such as, but not limited to, CAMCOG) with confluent white matter hyperintensities on MRI (defined as Fazekas $\geq 2$ )	<ul style="list-style-type: none"> <li>- Evidence for a monogenic form of SVDs</li> <li>- In case of inclusion for clinical lacunar stroke: <math>\geq 50\%</math> luminal stenosis in large arteries supplying the infarct area</li> <li>- Major-risk for cardioembolic source of embolism (defined as permanent or paroxysmal atrial fibrillation, sustained atrial flutter, intracardiac thrombus, prosthetic cardiac valve, atrial myxoma or other cardiac tumors, mitral stenosis, myocardial infarction in the last 4 weeks, left ventricular ejection fraction <math>&lt; 30\%</math>, valvular vegetations, or infective endocarditis)</li> <li>- Other specific causes of stroke (e.g. arteritis, dissection, vasospasm, drug misuse)</li> </ul>
<b>Additional selection criteria specific to patients with CADASIL</b>	
<b>Inclusion criteria</b>	<b>Exclusion criteria</b>
A diagnosis of CADASIL established by molecular genetic testing of the <i>NOTCH3</i> gene (presence of an archetypical, cysteine-affecting mutation) or the presence of granular osmiophilic material in ultrastructural, electron microscopy analysis of skin biopsy. <i>NB: thus both symptomatic and asymptomatic patients are included.</i>	Not applicable
<b>Additional selection criteria specific to controls</b>	
<b>Inclusion criteria</b>	<b>Exclusion criteria</b>
No additional inclusion criteria applicable	<ul style="list-style-type: none"> <li>- A history of stroke or of cognitive complaints for which the person has previously sought medical advice</li> <li>- So-called "silent" SVDs defined as confluent white matter hyperintensities (Fazekas <math>\geq 2</math>) or lacunes on the 3T brain MRI scan on baseline visit 1</li> </ul>

TREAT-SVDs) and the analyses and findings will be combined for all three studies and addressed in separate work.

#### 2.4.3. Blood pressure monitoring at home

At baseline, participants receive a telemetric blood pressure device to measure their blood pressure at home for seven days. The device

(Tel-O-Graph® GSM Plus) has a CE 0044 label, has been validated according to the European standard ISO 81,060–2:2009 and is graded A/A by the British Hypertension Society. Data are anonymously transferred via mobile phone networks (GPRS, General Packet Radio Service) to a central database for analysis. Participants measure the blood pressure three times daily: after waking, at noon and in the evening at bedtime.

**Table 3**

Neuropsychological tests and questionnaires in fixed order. MMSE= Mini-Mental State Examination, CES-D= Center for Epidemiological Studies Depression Scale.

Neuropsychological tests	Cognitive function	Cognitive domain
Category fluency (animals, 60 s)	Verbal fluency, semantic memory	Executive function
Boston naming test (short version)	Word naming	Language
MMSE	Cognitive screening	-
Word List Learning		
Immediate recall	Episodic memory	Memory
Delayed recall	Episodic memory	Memory
Delayed recognition	Episodic memory	Memory
Constructional praxis		
Copy	Visuoconstruction	Visuoconstruction
Delayed recall	Visuospatial memory, visuoconstruction	Memory
Trail making test		
Part A	Attention and psychomotor speed	Attention and processing speed
Part B	Executive function	Executive function
Phonemic fluency (letter S, 60 s)	Verbal fluency, executive function	Executive function
Digit span		
Forward	Attention and information processing speed	Attention and processing speed
Backward	Working memory	Executive function
<b>Questionnaires</b>	<b>Scope</b>	
Clinical Dementia Rating scale	Cognitive screening questionnaire	
CES-D questionnaire	Depressive symptoms questionnaire	

Participants are instructed to repeat the blood pressure measurements at each time point within 5 min. For data analyses, only the 2nd blood pressure measurement is used. If only one reading at a time point is available, that data will be used for the analysis. In addition to blood pressure, a pulse wave analysis is automatically performed with each blood pressure measurement to assess pulse wave velocity.

#### 2.4.4. Neuropsychological assessment

All participants undergo a standardized neuropsychological assessment battery in a fixed order. The battery includes the Consortium to Establish a Registry for Alzheimer's Disease (CERAD) battery [16], with the addition of the Trail Making Test [17], phonemic fluency [17], and digit span [18] to better assess processing speed and executive function (Table 3). The battery is concise, but still covers global cognition as well as specific cognitive domains. Individual test scores are standardized into *z*-scores using the control groups as a reference. Test *z*-scores are combined to represent specific cognitive domains (Table 3). Subsequently, global cognitive functioning is calculated as an average *z*-score across all domains. In addition, a clinical dementia rating scale (CDR) is obtained [19] and depressive symptoms are assessed with the Center for Epidemiologic Studies Depression Scale (CES-D) [20]. The main cognitive outcome will be a compound score of the *z*-scores for the domains attention and processing speed, and executive function.

#### 2.4.5. 3T brain mri

3T brain MRI data are acquired on a Philips Achieva 3T scanner with an 8-channel SENSE head coil at UMCU (patients with sporadic SVD and controls) and on a Siemens Magnetom Skyra 3T scanner with a 64 channel head coil at the LMU (patients with CADASIL and controls). The scan protocol includes a 3D T1-weighted gradient echo, a 3D T2-weighted turbo spin echo, a 3D T2\*-weighted gradient echo, and a 3D fluid-attenuated inversion recovery (FLAIR) scan. These sequences serve to assess conventional markers of SVDs and global brain volumes. In addition, the scan protocol includes diffusion imaging to measure white matter integrity. Table 4 summarizes all sequences and technical details for both sites.

SVD markers – i.e. lacunes, microbleeds and perivascular spaces – are visually rated on the 3T MRI scans by two trained raters according to the STRIVE criteria [3]. Differences between raters are resolved by consensus.

Volumetric measures are determined with established protocols at the individual study sites, to ensure that the data are analyzed with the

best suiting software for the scanner systems and participant populations. At the UMCU, white matter hyperintensities (WMHs) are automatically segmented from T1-weighted and FLAIR images [21,22], manually checked and, if necessary, edited. Lacunes are manually segmented using intensity-based seed-growing in an in-house built tool in MeVis-Lab (MeVis Medical Solutions AG, Bremen, Germany). T1-weighted images and FLAIR images are automatically segmented with the Computational Anatomy Toolbox (CAT12 <http://www.neuro.uni-jena.de/cat/>) to generate tissue probability maps from which gray matter (GM), white matter (WM) and cerebrospinal fluid (CSF) volumes are approximated. GM and WM volumes are normalized for intracranial volume. At the LMU, volumetric measures are assessed as previously published [23]. In short, WMHs are automatically segmented using a deep learning algorithm [24,25], manually checked, and edited when necessary. Lacunes are manually segmented using intensity-based seed-growing in a custom 3D editing tool in MATLAB (R2016b, The MathWorks, Natick, MA). Total intracranial and brain volumes are approximated from tissue probability maps calculated from the T1-weighted images, using SPM (v12; Wellcome Department of Cognitive Neurology, London, UK; <http://www.fil.ion.ucl.ac.uk/spm>). GM and WM volumes are normalized for intracranial volume.

#### 2.4.6. 7T brain mri

All 7T brain MRI data are acquired on a Philips 7T scanner at the UMCU (Philips Healthcare, Best, The Netherlands) using a 32-channel receive head coil in combination with a quadrature transmit coil (Nova Medical, MA, USA). 7T MRI offers three main advantages over regular field strength imaging for studying small vessel function [26]: (1) higher signal to noise ratio allowing for high spatial and temporal resolution measurements, (2) higher sensitivity to the magnetic susceptibility effect of deoxyhemoglobin responsible for the blood oxygenation level-dependent (BOLD) MR contrast and (3) improved ability to discern the BOLD signal in the small vessels from that in larger draining veins.

In ZOOM@SVDs, we use three dedicated 7T protocols that can inform about small vessel function:

- 1 Blood flow velocity and flow pulsatility are assessed in perforating arteries in the basal ganglia and semioval centre with dedicated 2D phase-contrast velocity mapping [27–29]. These measures assess flow in the perforating arteries in a 2D slice at the level of the basal ganglia and semioval centre. The measures are influenced by the state of the perforating arteries, but also by up- and downstream flow regulation.

**Table 4**

3T brain MRI protocol. GE= gradient echo; TSE= turbo spin echo; FLAIR= Fluid attenuated inversion recovery; DTI= diffusion tensor imaging; BOLD= Blood oxygenation level-dependent; rs-fMRI= resting state functional magnetic resonance imaging; Qflow = quantitative flow; (pC)ASL= (pseudoContinuous) Arterial spin labeling; SWI= susceptibility weighted imaging; FOV= Field of view; TE= Echo Time; TI= Inversion Time; TR= Repetition Time.

MR sequence	Acquired resolution mm <sup>3</sup>	Time min:s	Parameters
<b>Utrecht</b>			
T1-weighted GE	1.0 × 1.0 × 1.0	05:39	FOV 256 × 232 × 192 mm <sup>3</sup> ; TR 8 ms; TI 955 ms; shot interval 2500 ms; flip angle 7°
T2-weighted TSE	0.7 × 0.7 × 0.7	07:37	FOV 250 × 250 × 190 mm <sup>3</sup> ; TR 2500 ms; TE 298 ms
T2*-weighted GE	0.8 × 0.8 × 0.8	02:22	FOV 230 × 192 × 144 mm <sup>3</sup> ; TR 69 ms; TE 29 ms; flip angle 23°
FLAIR	1.0 × 1.0 × 1.0	06:15	FOV 250 × 250 × 180 mm <sup>3</sup> ; TR 5000 ms; TE 253 ms; TI 1700 ms
Diffusion MRI	2.5 × 2.5 × 2.5	06:49	FOV 220 × 220 × 120 mm <sup>3</sup> ; TR 8185 ms; TE 73 ms; b-values 0 and 1200 s/mm <sup>2</sup> ; directions 45
BOLD rs-fMRI	2.9 × 2.9 × 3.5	05:00	FOV 200 × 235 × 146 mm <sup>3</sup> ; TR 2500 ms; 3 echos at TE 9.1, 25.3, and 41.4 ms [45]
Qflow	1.2 × 1.2 × 2.0	00:19	FOV 150 × 103 mm <sup>2</sup> ; TR 14 ms; TE 3.7 ms; flip angle 25°; Venc 100 cm/s
ASL	3.0 × 3.1 × 7.0	06:00	FOV 240 × 240 × 133 mm <sup>3</sup> ; pCASL; label duration 1800 ms; postlabeling delay 1800 ms; 40 dynamics
<b>Munich</b>			
T1-weighted GE	1.0 × 1.0 × 1.0	05:08	FOV 256 × 256 × 192 mm <sup>3</sup> ; TR 2500 ms; TE 4.37 ms; TI 1100 ms; flip angle 7°
T2-weighted TSE	0.9 × 0.9 × 0.9	03:42	FOV 263 × 350 × 350 mm <sup>3</sup> ; TR 3200 ms; TE 408 ms
T2*-weighted GE	0.9 × 0.9 × 2.0	05:56	FOV 230 × 160 × 187 mm <sup>3</sup> ; TR 35 ms; TE 5–30 ms; flip angle 15°
SWI	0.6 × 0.6 × 3.0	04:02	FOV 240 × 156 × 195 mm <sup>3</sup> ; TR 28 ms; TE 20 ms; flip angle 9°
FLAIR	1.0 × 1.0 × 1.0	06:27	FOV 250 × 250 × 176 mm <sup>3</sup> ; TR 5000 ms; TE 398 ms; TI 1800 ms
Diffusion MRI	2.0 × 2.0 × 2.0	07:47	FOV 240 × 150 × 240 mm <sup>3</sup> ; TR 3800 ms; TE 104.8 ms; b-values 0, 1000 and 2000 s/mm <sup>2</sup> ; 90 diffusion directions (30 for b = 1000 s/mm <sup>2</sup> and 60 for b = 2000 s/mm <sup>2</sup> )

2 Small vessel reactivity in the visual cortex in response to a visual stimulus (i.e. neurovascular coupling) is assessed by means of the BOLD hemodynamic response. This is an ROI based measure in the visual cortex that assesses the parenchymal microvasculature. Neuronal activation triggers neurovascular coupling and induces vasodilation through the capillaries in the feeding pre-cappillary, parenchymal and penetrating arterioles to increase blood flow to the activated visual cortex [30].

3 Whole-brain small vessel reactivity (cerebrovascular reactivity) to a hypercapnic stimulus (i.e. breathing 6% CO<sub>2</sub> in air) is measured with the BOLD response. This is a whole-brain measure from which more specific ROIs can be defined to assess the local parenchymal microvasculature. The hypercapnic stimulus causes relaxation of the vascular smooth muscle cells at the level of the arterioles, thereby causing direct small vessel vasodilation [31].

The three protocols are complementary as they assess different small vessel populations, in different ROIs, either at rest or during stimulation with two different types of stimuli. The next three paragraphs describe the methods of these three 7T MRI protocols.

#### 2.4.7. Blood flow velocity and pulsatility index in perforating arteries

Perforating artery flow data are acquired using two single-slice 2D phase-contrast acquisitions. Slices are placed at the level of the basal ganglia and the semioval centre using predefined anatomical landmarks [27]. A peripheral pulse unit is used for retrospective cardiac gating (Table 5 summarizes technical details). For post-processing, the ROI in the basal ganglia slice is manually delineated from the 2D phase-contrast magnitude image. The ROI in the semioval centre slice is generated using an automatically delineated 2D white matter mask from a T1-weighted scan. The outside border of this mask (80 pixels = 14 mm) is excluded to be robust to subject motion between the acquisition of the T1-weighted and the 2D phase-contrast scan, which could lead to unsolicited inclusion of cortical vessels located in sulci. In these ROIs, perforating artery detection is performed with a previously developed method which automatically excludes perforating arteries in ghosting artefacts in the semioval centre [32] and perforating arteries in the basal ganglia that are oriented non-perpendicularly to the scanning plane. Additionally, apparent perforating arteries that are located within a 1.2 mm radius from each other are excluded, as these mostly are 'false detections' of larger and non-perpendicular vessels. Subsequently, the perforating artery flow is assessed per subject as in earlier work [27,29,33]. The protocol is visually summarized in Fig. 1.

Outcome measures, assessed separately for the basal ganglia and the semioval centre, are cerebral perforating artery density (number of perforating arteries/cm<sup>2</sup>), mean blood flow velocity (the averaged mean velocity per subject in cm/s) and flow pulsatility index (PI). To determine PI, the perforating arteries' velocities over the cardiac cycle are first normalized and averaged. Then PI is calculated per subject as  $\frac{V_{max}-V_{min}}{V_{mean}}$  where V<sub>max</sub>, V<sub>min</sub> and V<sub>mean</sub> are the maximum, minimum and mean of the normalized and averaged blood flow velocity over the cardiac cycle [27,28]. For ZOOM@SVDs we consider PI and mean blood flow velocity as primary outcome measures.

#### 2.4.8. Small vessel reactivity to a visual stimulus

Participants are presented with a strong visual stimulus to activate the visual cortex, and the subsequent increase in oxygenated blood to the activated brain is measured through a BOLD contrast weighted sequence. By making a fit of the average hemodynamic response function (HRF) in response to the stimulus, we can study the amplitude, and timing of small vessel reactivity in the cortex.

BOLD MRI data are acquired in eight slices in the visual cortex during a 10-minute experiment (Table 5 summarizes technical details of the sequence). The visual stimulus is an 8 Hz blue-yellow reversing checkerboard, presented with Presentation software (Presentation® version 18.1, Neurobehavioral Systems, Inc). The stimulus train comprises a block design part to determine the region of interest, and an event-related design part to derive the HRF [34]. The experiment starts with the event-related design which consists of a baseline period of 45.1 s (= 51 vol), a trigger period of 413.6 s (= 470 vol) and another baseline period of 59.8 s (= 68 vol). During the baseline period, a black screen with two red dots is presented to serve as a fixation point. During the trigger period, a total of 51 stimuli of 500 ms each are presented (2 × 2 125 ms opposing checkerboard frames). The inter-stimulus interval range is 3.3–18.7 s, sampled from an exponential distribution, and uniform jittering of  $\frac{1}{4} \cdot TR$  is applied (yielding a sub-TR temporal resolution of 220 ms) [34,35]. The block design consists of blocks of 16.72 s (=19 vol) in which the fixation screen and reversing checkerboard are alternated over three blocks (total of 100.32 s = 114 vol). Within the ROI we disentangle signal from the small vessels and from larger draining veins based on signal properties: large draining veins have a low signal and high signal variability wherefore we can calculate a temporal noise-to-signal ratio per voxel and then apply a single fixed value threshold above which the voxel represents signal from a large vein. The protocol is visually summarized in Fig. 2A.



**Table 5**

7T brain MRI protocol in fixed order. CSO= Semioval centre; BG= Basal Ganglia; M1= first segment of the middle cerebral artery; BOLD= Blood oxygenation level-dependent; fMRI= functional magnetic resonance imaging; FOV= Field of view; TE= Echo Time; TI= Inversion Time; TR= Repetition Time. \*Total scan time for a heart rate of 80 bpm.

MR sequence	Acquired resolution mm <sup>3</sup>	Time min:s	Parameters
T1-weighted	1.0 × 1.0 × 1.0	01:59	FOV 250 × 250 × 190 mm <sup>3</sup> ; TR 4.2 ms; TI 1297 ms; shot interval 3000 ms; flip angle 5°
2D-Qflow CSO	0.3 × 0.3 × 2.0	03:24*	FOV 230 × 230 mm <sup>2</sup> ; reconstructed resolution 0.18 × 0.18 mm [2]; TR 29 ms; TE 16 ms; Venc 4 cm/s
T1-weighted <sup>a</sup>	1.0 × 1.0 × 1.0	00:47	FOV 250 × 250 × 190; TR 4.1 ms; TI 1253 ms; shot interval 3000; flip angle 5°
2D-Qflow BG	0.3 × 0.3 × 2.0	03:47*	FOV 170 × 170 mm <sup>2</sup> ; reconstructed resolution 0.18 × 0.18 mm <sup>2</sup> ; TR 28 ms; TE 15 ms; Venc 20 cm/s
2D-Qflow M1	0.5 × 0.5 × 3.0	01:47*	FOV 250 × 200 mm <sup>2</sup> ; TR 12 ms; TE 4.3 ms; Venc 100 cm/s
T2* whole brain	0.6 × 0.6 × 0.6	03:02	FOV 239 × 191 × 100 mm <sup>3</sup> ; TR 77 ms; TE 27 ms; flip angle 20°
T2* visual cortex	0.6 × 0.6 × 1.0	02:21	FOV 160 × 169 × 29 mm <sup>3</sup> ; TR 1250 ms; TE 16 ms; flip angle 40°
BOLD fMRI visual cortex <sup>b</sup>	1.3 × 1.3 × 1.3	10:05	FOV 140 × 140 × 11 mm <sup>3</sup> ; TR 880 ms; TE 25 ms
T1-weighted <sup>a</sup>	1.0 × 1.0 × 1.0	00:47	FOV 250 × 250 × 190 mm <sup>3</sup> ; TR 4.1 ms; TI 1253 ms; shot interval 3000; flip angle 5°
BOLD fMRI whole-brain <sup>c</sup>	2.0 × 2.0 × 2.0	10:00	FOV 224 × 256 × 101 mm <sup>3</sup> ; TR 3000 ms; TE 25 ms

<sup>a</sup> A fast version of the T1-weighted sequence was added multiple times to assess potential subject motion during the scan, particularly after repositioning for attaching the mask for the hypercapnic challenge.

<sup>b</sup> The participant is presented with a visual stimulus.

<sup>c</sup> The participant undergoes a hypercapnic challenge.

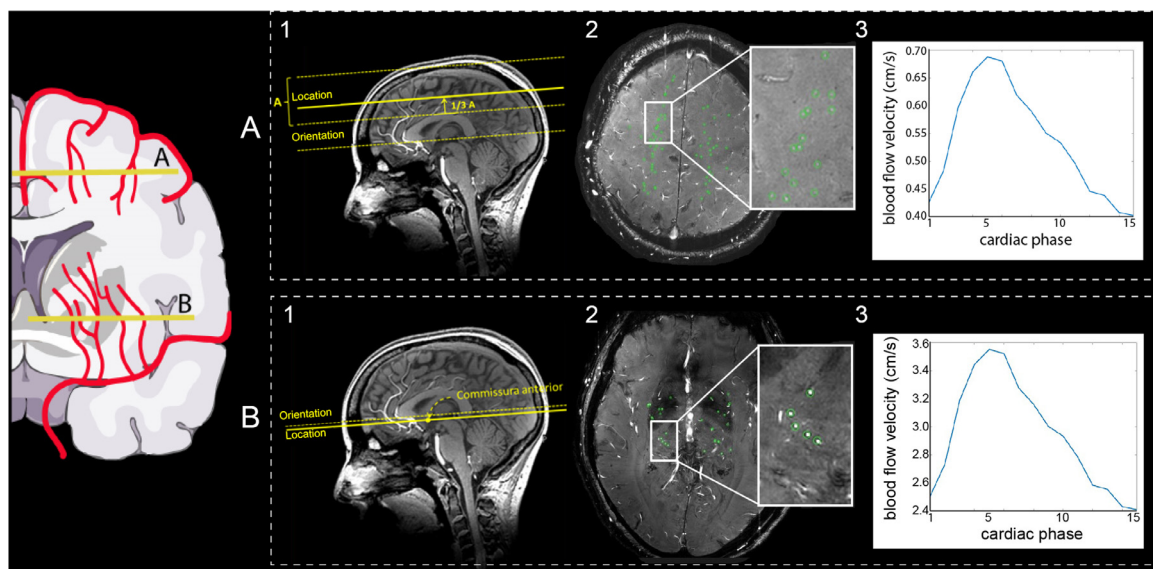


**Fig. 1.** Overview figure of the single-slice 2D phase-contrast acquisitions. The schematic image on the left provides an impression of the perforating arteries that are assessed. Part A and B show examples of the (1) image acquisition, (2) 2D slice with the perforating arteries in green in the regions of interest, and (3) a blood flow velocity trace for the semioval centre (A) and the basal ganglia (B) respectively. From the blood flow velocity trace, an average blood flow velocity and flow pulsatility index are calculated.

Outcome measures for the block design are ROI volume and BOLD amplitude. Outcome measures for the event-related design are four HRF characteristics: amplitude, full-width-at-half-maximum (FWHM), onset time and time-to-peak, separately for both the small vessels and the larger draining veins within the ROI. For ZOOM@SVDs we consider HRF amplitude and FWHM in the small vessels as primary outcome measures.

#### 2.4.9. Small vessel reactivity to a hypercapnic stimulus

Whole-brain cerebrovascular reactivity was measured using BOLD contrast weighted MRI during a 10-minute experiment (Table 5 summarizes the sequence's technical details). The vasoactive stimulus is a hypercapnic challenge based on an earlier published protocol in SVDs [36]. In short, participants wear a face mask connected to a unidirectional breathing circuit. The participants breathe medical air and 6% CO<sub>2</sub> in air with a flow rate of 30 L/min in alternating two-minute blocks: three two-minute blocks of medical air with two two-minute blocks of 6% CO<sub>2</sub> in air in between. Gasses are pre-mixed in medically graded cylinders (Linde Gas, The Netherlands). Monitoring equipment records

pulse rate (sampling rate = 500 Hz) and end-tidal CO<sub>2</sub> (etCO<sub>2</sub>, 40 Hz; CD3-A AEI Technologies, Pittsburgh, USA). The protocol is visually summarized in Fig. 2B.

Outcome measures are the BOLD response amplitude in the cortical and subcortical GM, and total WM, NAWM and WMH. For ZOOM@SVDs, we consider the BOLD response amplitude in all these ROIs as primary outcome measures.

#### 2.5. Follow up assessment

Two years after the baseline visit, all participants are invited for follow-up. During this visit, the clinical assessment, neuropsychological assessment (same test versions as at baseline) and 3T brain MRI scan are repeated (see Table 1 and respective sections above). If participants are not able to undergo a visit in the hospital, a short evaluation is performed via a telephone interview. If there is doubt about the reliability of the patient report because of cognitive problems, additional informa-

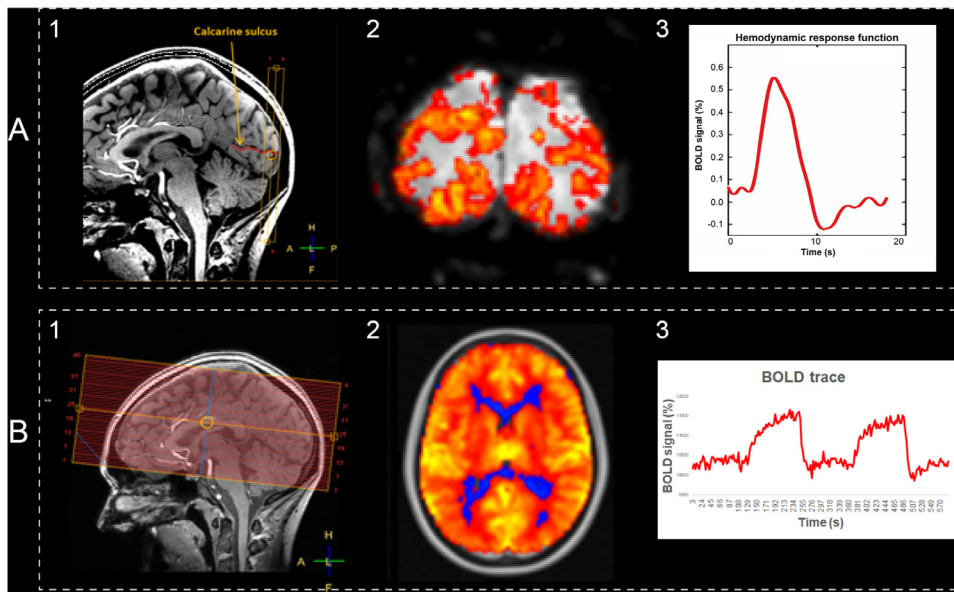


**Fig. 2.** Overview figure of the BOLD acquisitions. Part A (visual stimulus) and B (hypercapnic stimulus) show examples of the (1) image acquisition, (2) voxelwise reactivity maps, and (3) BOLD signal curves over time for small vessel reactivity. For A, amplitude and full-width-at-half-maximum are extracted from the hemodynamic response function. For B, the average% of BOLD signal change to the hypercapnic stimulus is calculated, using the recorded  $\text{etCO}_2$  trace as the input model for analysis.

tion is gathered from next of kin. Study participation finishes after the follow-up visit.

## 2.6. Sample size considerations

With a sample size of 60 patients with sporadic SVDs and 30 age and sex-matched controls, we can detect baseline abnormalities of small vessel function on continuous outcome measures with an effect size of 0.5 or more between groups with a power of 80% at a 5% significance level. At two-year follow-up, we expect that the dropout rate will not exceed 20%. This means that we can detect associations between baseline small vessel function and lesion progression or cognitive decline over two years if the determinant explains 16% or more variance with a power of 80% at a 5% significance level.

Regarding the 20 CADASIL patients with their 10 age and sex-matched controls, we can detect abnormalities of small vessel function with an effect size of 0.96 or more between groups with a power of 80% at a 5% significance level. The average age of the CADASIL participants in the study is around 50 years. At this age, CADASIL patients already have marked manifestations of SVDs. In controls of this age, none or only very subtle manifestations of sporadic SVDs are to be expected. If CADASIL indeed manifests with abnormalities of small vessel function on 7T MRI, there should be substantial differences between the groups, for which the sample size should be sufficient.

## 2.7. Planned analyses

For the primary objective – to assess which aspects of small vessel function on 7T brain MRI are affected in patients versus controls –, cross-sectional analyses will be performed at baseline to compare patients with CADASIL or sporadic SVDs to their respective controls. Main outcome measures are compared between patients and controls with the appropriate parametric or non-parametric independent samples tests, adjusting for age and sex.

For the secondary objective – to assess how small vessel function relates to SVD disease severity at baseline and disease progression after two years –, analyses will primarily be performed within the patient groups. Measures of small vessel function will be related with baseline parenchymal SVD markers and cognitive functioning, and the progression of these indicators of disease severity at follow-up. Analyses will be performed with multiple regression and will be adjusted for age sex and vascular risk factors where appropriate.

## 2.8. Timeline

The first participant was enrolled in March 2017. Participant enrolment for the CADASIL patients and their age and sex-matched controls was completed in July 2019. Enrolment for the patients with sporadic SVDs and controls is still ongoing. We expect to publish the first baseline results in 2021. Two-year follow-up visits are ongoing.

## 3. Discussion

ZOOM@SVDs will provide novel functional biomarkers of SVDs at the level of the small vessels themselves. We will assess cerebral perforating artery flow, and vascular reactivity to a visual and a hypercapnic stimulus with 7T MRI in patients with hereditary (i.e. CADASIL) and sporadic SVDs and controls. The different protocols in ZOOM@SVDs capture complementary aspects of small vessel function; in different types of small vessels, in different ROIs, both at rest and during stimulation with two different types of stimuli. We will determine which aspects of small vessel function are affected by SVDs and how this relates to disease severity and progression.

The small vessel functional measures in ZOOM@SVDs were chosen based on their relevance for SVDs and earlier research. We assess blood flow velocity and pulsatility index in perforating arteries in the basal ganglia and semioval centre. These perforating arteries are of particular interest given that, in SVDs, these are affected by arteriolosclerosis. We interpret pulsatility index as a measure of vascular stiffness, but the measure is also influenced by up- and downstream cerebral blood flow, pulse pressure and autoregulation. In earlier explorative work, we reported higher pulsatility in perforating arteries of patients with stroke attributable to SVD compared with controls, but similar blood flow velocity [28]. In ZOOM@SVDs, we will expand these observations in larger cohorts of highly phenotyped patients, including patients with CADASIL as a prototypic condition of pure and relatively severe SVD. In addition, we assess small vessel reactivity through neurovascular coupling in the visual cortex. Earlier studies with similar paradigms on 3T MRI have observed decreased vascular reactivity in response to a visual stimulus in patients with cerebral amyloid angiopathy (CAA) [37–41]. In ZOOM@SVDs, we study CADASIL and sporadic SVDs that show largely subcortical lesions, but might have abnormal cortical small vessel reactivity as well. The strength of 7T MRI is that we will be able to carefully isolate the signal from the parenchyma, derived from changes in blood oxygen levels in the local capillaries and draining venules, in response to upstream arteriolar dilation. It is important to realize that, in order

to represent neurovascular coupling and small vessel function, neuronal activation to the visual stimulus should be unaffected. We expect neuronal activation to be normal in CADASIL and sporadic SVD, as an earlier study reported normal cortical electrical potentials to a visual stimulus in patients with CADASIL and CAA [39]. Lastly, we assess small vessel reactivity with a hypercapnic stimulus that causes vasodilation in the arterioles [31]. Compared with the visual stimulus, the hypercapnic stimulus provides a whole-brain (rather than only cortical) measure of small vessel reactivity, that does not involve neurovascular coupling. Earlier studies used this paradigm on 3T MRI and observed that lower vascular reactivity was related to a higher burden of parenchymal SVD lesions in sporadic [42] and monogenic SVD [43]. In ZOOM@SVDs, we can capitalize on the high-resolution signal of 7T MRI to study local small vessel function, for example at the exact location of parenchymal lesions.

A strength of the ZOOM@SVDs study is that we will assess small vessel disease at its core, in the small vessels. By using three complementary measures across different brain regions we will be able to evaluate different aspects of small vessel function in different vessel subpopulations. By studying both monogenic and sporadic SVDs, we expect to find both shared and differential features of different forms of SVDs. Although downstream consequences of CADASIL and sporadic SVDs in the parenchyma show important similarities, there clearly are differences in the molecular and cellular pathways that affect the small vessels, likely with different signatures of vessel (dys)function. Moreover, in sporadic SVDs, vascular risk factors may differentially affect different vessel populations. Hypertension, for example, is known to most strongly affect the perforating arteries at the base of the brain, which are directly exposed to high pressure from the large arteries [44]. Finally, functional changes in different vessel populations may differentially affect the brain parenchyma. Therefore ZOOM@SVDs will also assess the interrelation between the nature of small vessel dysfunction and patterns of injury, also in longitudinal analyses. A limitation of ZOOM@SVDs is that, given the extensive protocol, there will likely be a relative overrepresentation of patients that are less affected (i.e. in earlier disease stages). Moreover, in order not to make the protocol too demanding, we prioritized detailed assessment of the primary parameters of interest. Consequently, some of the secondary clinical outcome measures are only assessed with screening tests with restricted sensitivity (e.g. assessment of motor performance and depression). Finally, 3T MRIs and their post-processing were performed at different centres for patients with CADASIL and sporadic SVDs. Importantly, the scans of the respective controls were always acquired on the same scanners as the patients. Although differences in scan acquisition and analysis may give rise to small differences in for example brain volume measurements, this should not impact the outcome of the study, because all primary analyses involving 3T parenchymal injury markers will be done within each patient group in comparison to their respective controls.

ZOOM@SVDs will characterize which small vessel function measures are affected in patients with CADASIL and sporadic SVDs compared with controls. Within the patient groups, we will establish which functional measures relate to disease severity (e.g. lesion burden and cognitive functioning). These markers could be well-suited to assist future etiological studies. In addition, the reversible nature of small vessel function makes the measures possibly potent outcome markers in intervention studies on candidate therapies that target the small vessels, thereby ultimately supporting the development of eagerly needed SVD treatment.

## Declarations

## Funding

ZOOM@SVDs is part of SVDs@target that has received funding from the European Union's Horizon 2020 research and innovative program under grant agreement No. 666,881.

This work is also supported by Vici Grant 918.16.616 from the Netherlands Organisation for Scientific Research (NWO) to G.J.B. MDi has received funding from the Vascular Dementia Research Foundation, the LMUExcellent Investitionsfond, and the DFG as part of the Munich Cluster for Systems Neurology (EXC 2145 SyNergy – ID 390,857,198). JJMZ has received funding from the European Research Council under the European Union's Seventh Framework Program (FP/2007–2013) / ERC Grant Agreement n. 841,865. FND received funding from the Stroke Association Garfield Weston Foundation and NRS Scotland.

## Informed consent

Written informed consent is obtained from all participants prior to enrollment in the study.

## Ethical approval

The Medical Ethics Review Committees of the UMCU and the LMU both approved the study (under number NL62090.041.17 and 17-088, respectively). The study is conducted in accordance with the declaration of Helsinki and the European law of General Data Protection Regulation.

## Acknowledgements

We would like to thank all participants who generously offer their time and energy for the purpose of this study. We acknowledge our colleagues at Diakonessenhuis for referring participants to the UMCU for study participation, and the help from Jenny Watchmaker and Annabel Groenberg in initial steps of setting up processing pipelines for the BOLD hypercapnic stimulus data.

## References

- [1] J.M. Wardlaw, C. Smith, M. Dichgans, Small vessel disease: mechanisms and clinical implications, *Lancet Neurol.* 18 (2019) 684–696.
- [2] S. Debette, S. Schilling, M.G. Duperron, S.C. Larsson, H.S. Markus, Clinical significance of magnetic resonance imaging markers of vascular brain injury: a systematic review and meta-analysis, *JAMA Neurol.* 76 (2019) 81–94.
- [3] J.M. Wardlaw, E.E. Smith, G.J. Biessels, C. Cordonnier, F. Fazekas, R. Frayne, et al., Neuroimaging standards for research into small vessel disease and its contribution to ageing and neurodegeneration, *Lancet Neurol.* 12 (2013) 822–838.
- [4] A.G.W. Van Norden, K.F. De Laat, E.J. Van Dijk, I.W.M. Van Uden, L.J.B. Van Oudheusden, R.A.R. Gons, et al., Diffusion tensor imaging and cognition in cerebral small vessel disease: the RUN DMC study, *Biochimica et Biophysica Acta - Mol. Basis Dis.* 1822 (2012) 401–407.
- [5] A.M. Tuladhar, A.G.W. Van Norden, K.F. De Laat, M.P. Zwiers, E.J. Van Dijk, D.G. Norris, et al., White matter integrity in small vessel disease is related to cognition, *NeuroImage: Clin.* 7 (2015) 518–524.
- [6] E. Baykara, B. Geserich, R. Adam, A.M. Tuladhar, J.M. Biesbroek, H.L. Koek, et al., A novel imaging marker for small vessel disease based on skeletonization of white matter tracts and diffusion histograms, *Ann. Neurol.* 80 (2016) 581–592.
- [7] M. Duering, M.J. Konieczny, S. Tiedt, E. Baykara, A.M. Tuladhar, E. van Leijsen, et al., Serum neurofilament light chain levels are related to small vessel disease burden, *J. Stroke* 20 (2018) 228–238.
- [8] L. Pantoni, Cerebral small vessel disease: from pathogenesis and clinical characteristics to therapeutic challenges, *Lancet Neurol.* 9 (2010) 689–701.
- [9] F. Dabertrand, C. Krøigaard, A.D. Bonev, E. Cognat, T. Dalsgaard, V. Domenga-Denier, et al., Potassium channelopathy-like defect underlies early-stage cerebrovascular dysfunction in a genetic model of small vessel disease, *Proc. Natl. Acad. Sci.* 112 (2015) E796–E805.
- [10] A. Joutel, M. Monet-leprêtre, C. Gosele, C. Baron-menguy, A. Hammes, S. Schmidt, et al., Cerebrovascular dysfunction and microcirculation rarefaction precede white matter lesions in a mouse genetic model of cerebral ischemic small vessel disease, *J. Clin. Invest.* 120 (2010) 433–445.
- [11] J.J.M. Zwanenburg, M.J.P. Van Osch, Targeting cerebral small vessel disease with MRI, *Stroke* 48 (2017) 3175–3182.
- [12] M. Pols, P.H.M. Peeters, M.C. Ocké, N. Slimani, H.B. Bueno-de-mesquita, H.J.A. Collette, Estimation of reproducibility and relative validity of the questions included in the EPIC physical activity questionnaire, *Int. J. Epidemiol.* 26 (1997) 181S–1189.
- [13] J.M. Guralnik, E.M. Simonsick, L. Ferrucci, R.J. Glynn, L.F. Berkman, D.G. Blazer, et al., A short physical performance battery assessing lower extremity function: association with self-reported disability and prediction of mortality and nursing home admission, *J. Gerontol.* 49 (1994) M85–M94.
- [14] G.A. Ortiz, R.L. SaacoNational Institutes of Health Stroke Scale (NIHSS), *Wiley Encyclopedia of Clinical Trials, National Institutes of Health Stroke Scale (NIHSS)*, 2008.



- [15] G. Hamot, W. Ammerlaan, C. Mathay, O. Kofanova, F. Betsou, Method validation for automated isolation of viable peripheral blood mononuclear cells, *Biopreservation Biobanking* 13 (2015) 152–163.
- [16] J.C. Morris, A. Heyman, R.C. Mohs, J.P. Hughes, G. Van Belle, G. Fillenbaum, et al., The Consortium to Establish a Registry for Alzheimer's Disease (CERAD). Part I. Clinical and neuropsychological assessment of Alzheimer's disease, *Neurology* 39 (1989) 1159–1165.
- [17] M.D. Lezak, D.B. Howieson, E.D. Bigler, D. Tranel, *Neuropsychological Assessment*, Oxford University Press, New York: NY, 2012.
- [18] D. Wechsler, *Wechsler Adult Intelligence Scale-Fourth Edition*, Pearson, San Antonio, TX, 2008.
- [19] J.C. Morris, *The Clinical Dementia Rating (CDR): current version and scoring rules*, *Neurology* 43 (1993) 2412.
- [20] P.M. Lewinsohn, J.R. Seeley, R.E. Roberts, N.B. Allen, Center for Epidemiological Studies-Depression Scale (CES-D) as a screening instrument for depression among community-residing older adults, *Psychol. Aging* 12 (1997) 277–287.
- [21] Camarasa R., Doué C., de Bruijne M., Dubost F. Segmentation of White Matter Hyperintensities with an Ensemble of Multi-Dimensional Convolutional Gated Recurrent Units. 2018. <https://wmh.isi.uu.nl/wp-content/uploads/2018/08/coroflo.pdf>.
- [22] H.J. Kuijf, M. Biesbroek, J. de Bresser, R. Heinen, S. Andermatt, M. Bento, et al., Standardized assessment of automatic segmentation of white matter hyperintensities and results of the WMH segmentation challenge, *IEEE Trans. Med. Imaging* 38 (2019) 2556–2568.
- [23] B. Gesierich, A.M. Tuladhar, A. ter Telgte, K. Wiegertjes, M.J. Konieczny, S. Finsterwalder, et al., Alterations and test-retest reliability of functional connectivity network measures in cerebral small vessel disease, *Hum. Brain Mapp.* 41 (2020) 2629–2641.
- [24] O. Ronneberger, P. Fischer, T. Brox, U-Net: convolutional networks for biomedical image segmentation, in: *Proceedings of the International Conference on Medical Image Computing and Computer-Assisted Intervention*, 2015.
- [25] J. Long, E. Shelhamer, T. Darrell, Fully convolutional networks for semantic segmentation, in: *Proceedings of the 2015 IEEE Conference on Computer Vision and Pattern Recognition (CVPR)*, 2015.
- [26] J.C.W. Siero, A. Bhogal, J.M. Jansma, Blood oxygenation level-dependent/functional magnetic resonance imaging: underpinnings, practice, and perspectives, *PET Clin.* 8 (2013) 329–344.
- [27] W.H. Bouvy, L.J. Geurts, H.J. Kuijf, P.R. Luijten, L.J. Kappelle, G.J. Biessels, et al., Assessment of blood flow velocity and pulsatility in cerebral perforating arteries with 7-T quantitative flow MRI, *NMR Biomed.* 29 (2015) 1295–1304.
- [28] L. Geurts, J.J.M. Zwanenburg, C.J.M. Klijn, P.R. Luijten, G.J. Biessels, Higher pulsatility in cerebral perforating arteries in patients with small vessel disease related stroke, a 7T MRI study, *Stroke* 50 (2019) 62–68.
- [29] T. Arts, J.C.W. Siero, G.J. Biessels, J.J.M. Zwanenburg, Automated assessment of cerebral arterial perforator function on 7T MRI, *J. Magn. Reson. Imaging* 53 (2020) 1–9.
- [30] C. Iadecola, The neurovascular unit coming of age: a journey through neurovascular coupling in health and disease, *Neuron* 96 (2017) 17–42.
- [31] P.N. Ainslie, J. Duffin, Integration of cerebrovascular CO<sub>2</sub> reactivity and chemoreflex control of breathing: mechanisms of regulation, measurement, and interpretation, *Am. J. Physiol. - Regul. Integr. Compar. Physiol.* 296 (2009).
- [32] Arts T., Siero J., Biessels G.J., Zwanenburg J. Method for vessel selection effects the outcome and reproducibility of velocity and pulsatility measures in cerebral penetrating arteries. In: *Proceedings of the Annual Meeting of the International Society of Magnetic Resonance Montreal*, 2019; p. #3264.
- [33] L. Geurts, G.J. Biessels, P. Luijten, J. Zwanenburg, Better and faster velocity pulsatility assessment in cerebral white matter perforating arteries with 7T quantitative flow MRI through improved slice profile, acquisition scheme, and postprocessing, *Magn. Reson. Med.* 79 (2018) 1473–1482.
- [34] J.C. Siero, N. Petridou, H. Hoogduin, P.R. Luijten, N.F. Ramsey, Cortical depth-dependent temporal dynamics of the BOLD response in the human brain, *J. Cerebr. Blood Flow Metab.* 31 (2011) 1999–2008.
- [35] J.C.W. Siero, N.F. Ramsey, H. Hoogduin, D.W.J. Klomp, P.R. Luijten, N. Petridou, BOLD specificity and dynamics evaluated in humans at 7 T: comparing gradient-echo and spin-echo hemodynamic responses, *PLoS One* 8 (2013) 1–8.
- [36] M.J. Thrippleton, Y. Shi, G. Blair, I. Hamilton, G. Waiter, C. Schwarzbauer, et al., Cerebrovascular reactivity measurement in cerebral small vessel disease: rationale and reproducibility of a protocol for MRI acquisition and image processing, *Int. J. Stroke* 13 (2018) 195–206.
- [37] R.J. Williams, B.G. Goodyear, S. Peca, C.R. McCreary, R. Frayne, E.E. Smith, et al., Identification of neurovascular changes associated with cerebral amyloid angiopathy from subject-specific hemodynamic response functions, *J. Cerebr. Blood Flow Metab.* 37 (2017) 3433–3445.
- [38] A. Dumas, G.A. Dierksen, M. Eng, M.E. Gurol, A. Halpin, S. Martinez-ramirez, et al., Functional MRI detection of vascular reactivity in cerebral amyloid angiopathy, *Ann. Neurol.* 72 (2012) 76–81.
- [39] I. Cheema, A.R. Switzer, C.R. McCreary, M.D. Hill, R. Frayne, B.G. Goodyear, et al., Functional magnetic resonance imaging responses in CADASIL, *J. Neurol. Sci.* 375 (2017) 248–254.
- [40] S. Peca, C.R. McCreary, E. Donaldson, G. Kumarpillai, K. Sanchez, A. Charlton, et al., Neurovascular decoupling is associated with severity of cerebral amyloid angiopathy, *Neurology* 81 (2013) 1659–1665.
- [41] A.M. Van Opstal, S. Van Rooden, T. Van Harten, G. Labadie, P. Fotiadis, M.E. Gurol, et al., Cerebrovascular function in pre-symptomatic and symptomatic individuals with hereditary cerebral amyloid angiopathy: a case-control study, *Lancet Neurol.* 16 (2017) 115–122.
- [42] G.W. Blair, M.J. Thrippleton, Y. Shi, I. Hamilton, M. Stringer, F. Chappell, et al., Intracranial hemodynamic relationships in patients with cerebral small vessel disease, *Neurology* 94 (2020) e2258–e2269.
- [43] F.C. Moreton, B. Cullen, C. Delles, C. Santosh, R.L. Gonzalez, K. Dani, et al., Vasoreactivity in CADASIL: comparison to structural MRI and neuropsychology, *J. Cerebr. Blood Flow Metab.* 38 (2018) 1085–1095.
- [44] J.D. Spence, Blood pressure gradients in the brain: their importance to understanding pathogenesis of cerebral small vessel disease, *Brain Sci.* 9 (2019) 1–8.
- [45] P. Kundu, S.J. Inati, J.W. Evans, W.M. Luh, P.A. Bandettini, Differentiating BOLD and non-BOLD signals in fMRI time series using multi-echo EPI, *Neuroimage* 60 (2012) 1759–1770.